Discrete & Continuous Models & Applied Computational Science
ISSN 2658-7149 (Online), 2658-4670 (Print)

2026, 34 (1) 125–138
http://journals.rudn.ru/miph

Research article

UDC 537.527,533.9.03
PACS 52.80 Pi, 52.80.Sm, 52.50.Sw, 52.40.Db
DOI: 10.22363/2658-4670-2026-34-1-125-138 EDN: UOSEFX

Mathematical models of low-pressure discharge in a magnetic field supported by UHF electromagnetic field

Sergey A. Dvinin[1, 2], Denis V. Chuprov[2], Konstantin N. Kornev[1, 2], Zafari A. Qodirzoda[3], Davlat K. Solikhzoda[3]

[1] RUDN University, 6 Miklukho-Maklaya St, Moscow, 117198, Russian Federation

[2] Lomonosov Moscow State University 1 build 2 Leninskiye gory, Moscow, 119991, Russian Federation

[3] Tajik National University, 17 Rudaki Av, Dushanbe, 973402, Tajikistan

(received: February 6, 2026; revised: February 22, 2026; accepted: February 25, 2026)

Abstract. Electron cyclotron resonance (ECR) discharges are an effective way to generate plasma at low working gas pressure. The aim of this work is to develop a mathematical model of the ECR discharge implemented at the RAPIRA facility (RUDN University), which is used for a wide range of scientific research. The evolution of plasma particles is described within the framework of the hydrodynamic approximation (a two-dimensional model with cylindrical symmetry). A three-dimensional model of cold plasma is used to calculate the spatial distribution of the electromagnetic field. Calculations have shown that in the operating mode of the facility (gas pressures from $4 \cdot 10^{-4}$ to 10^{-2} Torr, magnetic field up to 2500 G), the electron temperature is equalized along the magnetic field lines, and at the same time, the magnetic field ensures a decrease in energy losses to the side walls of the facility. The spatial distributions of the electron density and temperature and the electromagnetic field in the plasma are calculated. The implemented model can serve as a basis for developing a more advanced set of software codes that take into account the non-Maxwellian nature of the electron velocity distribution function, caused by the non-adiabatic nature of their heating in a non-uniform magnetic field.

Key words and phrases: ECR discharge, discharge in a resonator, discharge in a magnetic trap, drift-diffusion model

For citation: Dvinin, S. A., Chuprov, D. V., Kornev, K. N., Qodirzoda, Z. A., Solikhzoda, D. K. Mathematical models of low-pressure discharge in a magnetic field supported by UHF electromagnetic field. *Discrete and Continuous Models and Applied Computational Science* **34** (1), 125–138. doi: 10.22363/2658-4670-2026-34-1-125-138. edn: UOSEFX (2026).

1. Introduction

Electron cyclotron resonance (ECR) discharge is currently used in various fields of science and technology: plasma-chemistry installations for material processing [1–7], sources for multiply charged ions (MCI) [8–10], sources of hydrogen ions for proton accelerators [11, 12], and microwave plasma thruster [13]. The multitude of possible applications has led to a variety of discharge installation geometries in which ECR interaction is realized, differing both in the spatial configuration of the constant magnetic field and in the method of exciting the electromagnetic field and its frequencies. On the other hand, the diversity of installation options determines different approaches to constructing mathematical models of the processes occurring in these installations.

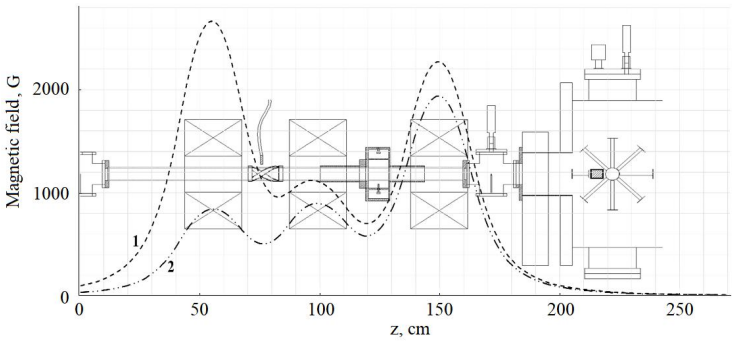

Figure 1. Setup diagram: A—processing chamber, B—quartz plasma pipeline, C—gas inlet connection point, D—helicon antenna, E—microwave resonator, F1, F2, F3—magnetic coils. Axial distribution of magnetic field induction along plasma pipeline under microwave (1) and HF (2) discharges

The purpose of this work is to formulate an approach for developing a model of microwave discharge implemented on the multifunctional installation—RAPIRA (Resonant Accelerated Plasma Installation Research & Application, RUDN University), used to study the absorption of microwave power by a magnetized plasma filling a cavity, the processes of plasma transport along a cylindrical quartz discharge tube (plasma pipeline) from the source to the processing chamber and processing of various chemical and biological objects by plasma created.

2. Experimental setup and computer modeling tools

The schematic view of the RAPIRA installation is shown in Figure 1. First of all, we list the elements and systems that are important and relevant for the numerical model being developed. The installation contains (A)—a processing chamber in which the processed samples are placed, (B)—a quartz plasma pipeline, (C)—a gas inlet system, (D)—helicon antenna for generation of RF (13.56 MHz) discharge, (F)—coils (1, 2, 3) for generating a magnetic field, and (E)—a microwave cavity. The magnetic field configuration is controlled by currents through coils (F.1–F.3).

The experimental setup was developed to use RF and microwave plasma discharges to create plasma flows to study their interaction with various substrates. The RF discharge is generated using a half-wave helicon antenna, the microwave discharge is initiated in a cylindrical resonator with the fundamental oscillation mode H_{111}. The curves of two longitudinal magnetic field distributions, providing resonant conditions during the operation of microwave 1 and RF 2 plasma sources, are also shown in figure 1. The range of possible pressures of the plasma-forming gases and mixtures of the installation is quite wide, but in this paper, we will consider the option of generating microwave plasma at 0.01–0.04 Pa. The microwave resonator is excited by two rod antennas inserted into the resonator perpendicular to the side wall. Each rod is 6 mm in diameter and inserted 32.1 mm deep of the cavity. An electrodynamic model for a microwave discharge is considered as an example for calculation. To prevent the loss of microwave radiation through the holes in the end walls of the cavity, the axisymmetric quartz pipeline was shielded with cylindrical evanescent waveguides.

The paper shows that in the specified pressure range (with the possible exception of the lowest pressures), the discharge can be described within the drift-diffusion model, including the particle balance equations, the energy balance equation, and Maxwell's equations. This approach is standard for most gas discharge models [14]. The specificity of this work is that this system of equations is

used to describe the discharge in a non-uniform magnetic field. The system of equations obtained below was solved using the Comsol Multiphysics software package [15]. The RF module of Comsol was used to solve the electrodynamic equations, and the diffusion and heat transfer equations were solved using the main module. The magnetic field of each coil was approximated as the field of the current flowing along a ring of radius R. The radius R was chosen in such a way as to approximate the experimentally obtained dependence of the magnetic field of each coil along the plasma guide axis as accurately as possible. The zero coordinate of the calculation problem corresponded to the position of the resonator exciters.

The model of a microwave discharge in the specified pressure range (with the possible exception of the lowest pressures) can be described in the framework of the drift-diffusion approach, which includes particle balance equations, energy balance equation, and Maxwell's equations. This approach is standard for most gas discharge models [14]. The specificity of this paper is that the above-mentioned system of equations is used to describe discharge in a non-uniform magnetic field. The system of equations was solved using the Comsol Multiphysics software package [15]. The specificity of this paper is that the system of equations is used to describe the discharge in a non-uniform magnetic field. The RF module of Comsol was used to solve the electrodynamic equations, and the drift-diffusion model equations were solved using the main module. The magnetic field of each coil was approximated as the field of the current flowing along a ring of radius R. The radius R was chosen in such a way as to approximate the experimentally obtained dependence of the magnetic field of each coil along the plasma guide axis as accurately as possible. The zero coordinate of the calculation problem corresponded to the position of the resonator exciters.

3. Diffusion and loss of particles in the discharge

Estimates show that the longitudinal dimensions of the plasma conduit in the pressure range of 0.01–0.04 Pa are greater than the wavelength, with the possible exception of the lowest pressures in this range. In the transverse direction, the magnetization conditions are satisfied: $|\Omega_\alpha|\tau_\alpha > 1$, where $\Omega_\alpha = e_\alpha B/m_\alpha c$, $\tau_\alpha^{-1} = \nu_\alpha$ is the cyclotron frequency and the collision frequency of type α particles ($\alpha = e$ for electrons and $\alpha = +$ for ions). In this case, the transverse discharge dimensions also exceed the Larmor radius, so the latter can be considered as the mean free path when considering the radial motion of charged particles. Therefore, in this case, the discharge can be described within the framework of the drift-diffusion (hydrodynamic) model.

In this case, the diffusion and thermal conductivity coefficients become anisotropic [16]. In a uniform magnetic field, the diffusion equations have the form:

$$n_e\mathbf{V}_e = -\frac{n_e}{1+(\Omega_e/\nu_{en})^2}\left\{\left(\mu_e\mathbf{E} + D_e\frac{\nabla n_e}{n_e}\right) + \left[\frac{e}{\nu_{en}}\times\left(-\mu_e\mathbf{E} - D_e\frac{\nabla n_e}{n_e}\right)\right]\right\} - \\ - \mu_e n_e\frac{e(\mathbf{E}_e)}{\Omega_e^2} - D_e\frac{e(\nabla n_{ee})}{\Omega_e^2}, \quad (1)$$

$$n_+\mathbf{V}_+ = \frac{n_+}{1+(\Omega_+/\nu_{+n})^2}\left\{\left(\mu_+\mathbf{E} - D_+\frac{\nabla n_+}{n_+}\right) + \left[\frac{+}{\nu_{+n}}\times\left(\mu_+\mathbf{E} - D_+\frac{\nabla n_+}{n_+}\right)\right]\right\} + \\ + \mu_+ n_+\frac{+(\mathbf{E}_+)}{\Omega_+^2} - D_+\frac{+(\nabla n_{++})}{\Omega_+^2}. \quad (2)$$

Here n_e, n_+, Ω_e, Ω_+ and ν_{en}, ν_{+n} are the densities, cyclotron frequencies and effective collision frequencies for electrons and ions, μ_e, μ_+, D_e, D_+ are the mobilities and diffusion coefficients of electrons and ions along the magnetic field, **E** is the ambipolar field. Thus, the magnetic field does not affect the motion of particles along the magnetic field lines. In addition, from equations (1) and (2) it follows that particles participate in drift motion in the direction perpendicular to both the electric and magnetic fields, with negative and positive particles drifting in different directions. Finally, there is drift and diffusion of particles in the direction parallel to the electric field and the density gradient of charged particles. The value of diffusion coefficients in the direction across the magnetic field are significantly smaller than the value, when particles moves along a magnetic field.

$$D_{e\perp} = \frac{D_e}{1+(\Omega_e/\nu_{en})^2}, \qquad D_{+\perp} = \frac{D_+}{1+(\Omega_+/\nu_{+n})^2},$$
$$\mu_{e\perp} = \frac{\mu_e}{1+(\Omega_e/\nu_{en})^2}, \qquad \mu_{+\perp} = \frac{\mu_+}{1+(\Omega_+/\nu_{+n})^2}.$$

The complete system of equations in the drift-diffusion model for a homogeneous magnetic field includes equations for the electron and ion currents (1), (2), and the electron and ion balance equations. The Poisson equation, which should close the system of equations, is replaced by the quasi-neutrality condition, whereby the equation for the electron density is excluded from consideration, and instead, the equation for the electric current is used, which is also a consequence of the quasi-neutrality condition: $n_+ = n_e = n$, $\left(\nabla \cdot n(\mathbf{V}_e - \mathbf{V}_+)\right) = 0$. Using equations (1) and (2), we also eliminate the equations for the electron and ion currents. Thus, the complete system of equations takes the form:

$$-\frac{\partial}{\partial z}\left(D_{+zz}\frac{\partial n}{\partial z} + n\mu_{+zz}\frac{\partial \varphi}{\partial z}\right) - \frac{\partial}{\partial x}\left(D_{+xx}\frac{\partial n}{\partial x} + n\mu_{+xx}\frac{\partial \varphi}{\partial x}\right) = \nu_i n, \tag{3}$$

$$\frac{\partial}{\partial z}\left((D_{ezz} - D_{+zz})\frac{\partial n}{\partial z} - n(\mu_{ezz} + \mu_{+zz})\frac{\partial \varphi}{\partial z}\right) + \frac{\partial}{\partial x}\left((D_{exx} - D_{+xx})\frac{\partial n}{\partial x} - n(\mu_{exx} + \mu_{+xx})\frac{\partial \varphi}{\partial x}\right) = 0. \tag{4}$$

The final system of equations for a system with one type of ion includes equations (3), (4). The boundary conditions are usually set in the form ($\boldsymbol{\eta}$ is the normal to the wall surface, Λ_i is the mean free path of the ion).

$$\left(\boldsymbol{\eta} \cdot \nabla n\right) = n/\Lambda_i, \qquad \left(\boldsymbol{\eta} \cdot (-\mathbf{j}_e + \mathbf{j}_+)\right) = 0. \tag{5}$$

Equations (5) are valid in the case when ion mean free path is less than the size of the sheath between the plasma and the quartz tube. Otherwise, the Bohm criterion is used, which states that the plasma flow velocity at the boundary is equal to the ion-sound velocity. The partial differential equations were solved using the Comsol Multiphysics mathematical package [15].

In a nonuniform magnetic field, the induction is not directed along the 0Z axis. Therefore, the diffusion and mobility tensors of charged particles will no longer be diagonal. Below we write the ion balance equation and the equations for the currents, which replace equations (3) and (4). Further in the formulas we replace n_e and n_+ by n.

1. Equation of charged particle densities (The upper sign + corresponds to ions, the lower sign − to electrons):

$$\frac{\partial n}{\partial t} - \frac{\partial}{\partial z}\Big[\left(D_{e,i\perp} - D_{e,i\parallel}\right)\sin\theta\cos\theta\frac{\partial n}{\partial r} - \left(D_{e,i\perp}\sin^2\theta + D_{e,i\parallel}\cos^2\theta\right)\frac{\partial n}{\partial z} \pm$$
$$\pm\, n\left(\mu_{e,i\perp} - \mu_{e,i\parallel}\right)\sin\theta\cos\theta\frac{\partial \varphi}{\partial r} \pm n\left(\mu_{e,i\perp}\sin^2\theta + \mu_{e,i\parallel}\cos^2\theta\right)\frac{\partial \varphi}{\partial z}\Big] -$$
$$-\frac{\partial}{r\partial r}\Big[\left(D_{e,i\perp}\cos^2\theta + D_{e,i\parallel}\sin^2\theta\right)r\frac{\partial n}{\partial r} - \left(D_{e,i\parallel} - D_{e,i\perp}\right)r\frac{\partial n}{\partial z}\sin\theta\cos\theta \pm$$

$$\pm n\left(\mu_{e,i\perp}\cos^2\theta + \mu_{e,i\parallel}\sin^2\theta\right)\frac{\partial\varphi}{\partial r} \pm n\left(\mu_{e,i\perp} - \mu_{e,i\parallel}\right)\frac{\partial\varphi}{\partial z}\sin\theta\cos\theta\Big] = \nu_i n.$$

2. Equations for the ambipolar field potential

$$\begin{aligned}(\nabla\cdot\mathbf{J}) = \frac{\partial}{\partial z}\Big\{&\Big(\left(D_{e\perp} - D_{i\perp}\right) - \left(D_{e\parallel} - D_{i\parallel}\right)\Big)\sin\theta\cos\theta\frac{\partial n}{\partial r} - \\ &- \left(\left(D_{e\perp} - D_{i\perp}\right)\sin^2\theta + \left(D_{e\parallel} - D_{i\parallel}\right)\cos^2\theta\right)\frac{\partial n}{\partial z} - \\ &- \Big(\left(\mu_{e\perp} - \mu_{i\perp}\right) - \left(\mu_{e\parallel} - \mu_{i\parallel}\right)\Big)\sin\theta\cos\theta\frac{\partial\varphi}{\partial r} - \\ &- \left(\left(\mu_{e\perp} - \mu_{i\perp}\right)\sin^2\theta + \left(\mu_{e\parallel} - \mu_{i\parallel}\right)\cos^2\theta\right)\frac{\partial\varphi}{\partial z}\Big\} - \\ -\frac{1}{r}\frac{\partial}{\partial r}r\Big\{&\left(\left(D_{e\perp} - D_{i\perp}\right)\cos^2\theta + \left(D_{e\parallel} - D_{i\parallel}\right)\sin^2\theta\right)\frac{\partial n}{\partial r} - \\ &- \Big(\left(D_{e\parallel} - D_{i\parallel}\right) - \left(D_{e\perp} - D_{i\perp}\right)\Big)\sin\theta\cos\theta\frac{\partial n}{\partial z} - \\ &- n\Big(\left(\mu_{e\perp} + \mu_{i\perp}\right)\cos^2\theta + \left(\mu_{e\parallel} + \mu_{i\parallel}\right)\sin^2\theta\Big)\frac{\partial\varphi}{\partial r} + \\ &+ n\Big(\left(\mu_{e\parallel} + \mu_{i\parallel}\right) - \left(\mu_{e\perp} + \mu_{i\perp}\right)\Big)\sin\theta\cos\theta\frac{\partial\varphi}{\partial z}\Big\} = 0. \quad (6)\end{aligned}$$

In these equations, θ is the angle between the direction of the constant magnetic field and the 0Z axis: $\theta = \arctan\left(H_r(r,z)/H_z(r,z)\right)$. The boundary conditions coincide with the conditions in a uniform magnetic field.

4. Heat transfer in the discharge. Heating and energy loss of electrons in the plasma

The charged particle balance equations include the electron and ion production rate, which depends on the chemical reactions occurring in the plasma. The rate of these reactions, in turn, depends on the electron temperature and the temperatures of the heavy particles. Since a low-pressure discharge is being considered, it can be expected that no temperature change along the field line should occur. In the transverse direction, where particle transport is suppressed by the magnetic field, energy transfer may be insufficient and the temperature may vary. Ideally, to calculate the frequencies of chemical processes, it is necessary to solve the heat conduction equation for electrons, which has the form

$$\begin{aligned}\frac{3}{2}nk\frac{\partial T_e}{\partial t} - \frac{\partial}{\partial z}\Big[&\left(\chi_{e\perp} - \chi_{e\parallel}\right)\sin\theta\cos\theta\frac{\partial T_e}{\partial r} - \left(\chi_{e\perp}\sin^2\theta + \chi_{e\parallel}\cos^2\theta\right)\frac{\partial n}{\partial z}\Big] - \\ &- \frac{\partial}{r\partial r}\Big[\left(\chi_{e\perp}\cos^2\theta + \chi_{e\parallel}\sin^2\theta\right)r\frac{\partial T_e}{\partial r} - \left(\chi_{e\perp} - \chi_{e\parallel}\right)r\frac{\partial T_e}{\partial z}\sin\theta\cos\theta\Big] = \\ &= \sum_{j=1}^{3}\sum_{i=1}^{3}\sigma_{ij}E_iE_j^* - Q. \quad (7)\end{aligned}$$

Here χ is the thermal conductivity coefficient of the plasma, which was calculated in accordance with [16, 17], k is Boltzmann constant. The role of the magnetic field was taken into account in accordance with [16]. Here $Q = nw_1$ is the energy transferred by electrons to other particles in elastic and inelastic collision. The calculation of w_1 will be discussed below. It can be expected that under the experimental conditions, due to the high thermal conductivity along the magnetic field lines, the electron temperature in this direction should equalize. Here, σ_{ij} is the plasma conductivity, accounting for its anisotropy and the high-frequency nature of the field. The field absorption is calculated using the effective collision frequency, which takes into consideration both collisional and collisionless energy gain by electrons.

In the direction perpendicular to the magnetic surface, the thermal conductivity of the electron gas is significantly lower, so radial temperature non-uniformity can be expected in cases where heating across the plasma cross-section is non-uniform. Therefore, the process of establishing the spatial distribution of electron temperature should be investigated using mathematical modeling.

According to models of a steady-state low-pressure discharge, ionization balances losses. Losses are determined by the discharge geometry (i.e., the position of the boundaries and the magnetic field strength profile), the chemical properties, and the pressure of the working gas. If the spatial distribution of electron temperature is uniform, then particle losses determine the ionization required in the discharge and, consequently, the electron temperature.

Then the value of this temperature should ensure particle balance, i.e., as is usually the case in a stationary discharge, the required temperature is determined by the particle balance. If the ionization cross-section is known, the temperature is determined from the relation

$$\nu_{i,s} = 4\pi N \int_0^\infty V q_{i,s}(V) f_e(V, T_e) V^2 \, dV, \tag{8}$$

where $q_{i,s}$ is the ionization or excitation cross-section, N is the density of neutral atoms, $f_e(V)$ is the electron energy distribution function, which is assumed to be isotropic. If the function is Maxwellian and a linear approximation is used for the process cross-section (ε_i is ionization threshold),

$$q_i = a(\varepsilon - \varepsilon_i), \tag{9}$$

or Fabrikant's approximation (ε_m is the energy at which the ionization cross-section is maximum and equal to q_m)

$$q_s = q_{ms} \frac{\varepsilon - \varepsilon_s}{\varepsilon_{ms} - \varepsilon_s} \exp\left(\frac{\varepsilon_{ms} - \varepsilon}{\varepsilon_{ms} - \varepsilon_s}\right),$$

then the following expressions can be obtained for the frequencies (e, m are electron charge and mass):

$$\nu_i = \frac{4}{\sqrt{\pi}} \left(aN \frac{kT_e}{e}\right) \left(\frac{2kT_e}{m}\right)^{1/2} \left(1 + \frac{\varepsilon_i}{2kT_e}\right) \exp\left(-\frac{\varepsilon_i}{kT_e}\right),$$

$$\nu_s = \frac{4}{\sqrt{\pi}} q_{ms} N \left(\frac{2kT_e}{m}\right)^{1/2} \frac{kT}{\varepsilon_{ms} - \varepsilon_s} \left[1 + \frac{\varepsilon_s}{2kT_e}\left(1 + \frac{kT_e}{\varepsilon_{ms} - \varepsilon_s}\right)\right] \times \exp\left(1 - \frac{\varepsilon_s}{kT_e}\right) \Big/ \left(1 + \frac{kT_e}{\varepsilon_{ms} - \varepsilon_s}\right)^3.$$

If more accurate results are required, approximations [18] and numerical integration (8) can be used. The energy losses of electrons are determined by the relation

$$w_1(T_e) = \frac{2m}{M} \nu_{en} \frac{3}{2} k(T_e - T_g) + \sum_s \nu_s(T_e) \varepsilon_s + \nu_i(T_e) \left(\varepsilon_i + 2kT_e + \varepsilon_{ist}\right).$$

The first term accounts for elastic energy losses, the second for excitation losses, and the third for ionization losses. The last term accounts for the energy carried away by ions toward the wall. Ion acceleration occurs due to the ambipolar field. The temperature distribution in the discharge is given by the thermal conductivity equation (7).

By integrating equation (7) over the entire discharge volume, we obtain the energy required to maintain a discharge with a given electron density. Note also that using cross-section (9) for the ionization frequency yields a temperature of 4.5 eV in the setup's operating modes, but the formula itself overestimates the ionization frequency. The energy required to create an electron under these conditions was 10^9 eV/s/Torr.

5. Spatial distribution of the electromagnetic field in the discharge

The particle balance equation (6) allows us to determine the ionization frequency (averaged over the volume) required to maintain the discharge at steady state. The particle balance equation (7) quantifies the energy required to create the required number of electrons in 1 second. Knowing this energy, we can determine the power required to maintain a plasma with a given average density n_0 by integrating the solution of equation (7) over the entire plasma volume:

$$W = \iiint\limits_V dx\, dy\, dz\, n_e(x, y, z) w_1(x, y, z).$$

The final step required to complete the mathematical model is to solve Maxwell's equations. Knowing the microwave power required to maintain the discharge allows us to determine the amplitude, spatial distribution of the microwave density, and discharge impedance, and select an appropriate method for matching the discharge to the generator. The model construction procedure described above is not self-consistent, since the solution of the particle balance equation assumed the electron temperature to be uniform throughout the volume, etc. Nevertheless, it usually allows for a fairly accurate determination of the averaged discharge parameters as functions of given conditions (geometry, chemical nature of the gas, etc.). The necessary refinement of the model can be made at later stages, possibly using well-developed perturbation theory or other methods.

Let us now turn to the presentation of the electrodynamic part of the problem. Electrodynamically, the discharge was described using the cold plasma model [19, 20]. Maxwell's equations were solved using the "Comsol Multiphysics" software package. The permittivity is written as:

$$(\varepsilon_{ij}) = \begin{pmatrix} \varepsilon_\perp & ig & 0 \\ -ig & \varepsilon_\perp & 0 \\ 0 & 0 & \varepsilon_\parallel \end{pmatrix},$$

where

$$\varepsilon_\perp = 1 - \frac{n_e}{n_c} \frac{(1 + i\nu_{en}/\omega)}{n_c(1 + i\nu_{en}/\omega)^2 - \Omega_e^2/\omega^2},$$
$$g = -\frac{n_e}{n_c} \frac{\Omega_e/\omega}{(1 + i\nu_{en}/\omega)^2 - \Omega_e^2/\omega^2},$$
$$\varepsilon_\parallel = 1 - \frac{n_e}{n_c} \frac{1}{1 + i\nu_{en}/\omega}.$$

Here $\omega_{Le} = \sqrt{4\pi ne^2/m}$ is the Langmuir frequency, n_e is the electron density, e and m are their charge and mass, ν_{en} is the effective electron collision frequency, and $_e = e\mathbf{B}_z/mc$ is the cyclotron frequency. In an inhomogeneous medium [21]

$$\hat{\varepsilon}_{ij} = \Phi^{-1}T^{-1}\begin{pmatrix} \varepsilon_\perp & ig & 0 \\ -ig & \varepsilon_\perp & 0 \\ 0 & 0 & \varepsilon_\parallel \end{pmatrix} T\Phi, \qquad T = \begin{pmatrix} \cos\theta & 0 & -\sin\theta \\ 0 & 1 & 0 \\ \sin\theta & 0 & \cos\theta \end{pmatrix},$$

$$\Phi = \begin{pmatrix} \cos\varphi & \sin\varphi & 0 \\ -\sin\varphi & \cos\varphi & 0 \\ 0 & 0 & 1 \end{pmatrix}.$$

The electrodynamic models used in the calculations differed in the geometry of the excitation system, the configuration of the magnetic field, the frequency of the microwave, and the frequency of electron-neutral collisions.

6. Simulation results and their discussion

The results of numerical modeling of the equations discussed above working gas argon, pressure $4 \cdot 10^{-4}$ Torr, spatial distribution of constant magnetic field corresponded to that measured in the experiment (Figure 1), describing the diffusion and drift of charged particles and heat transfer in plasma in cylindrical geometry (azimuth distribution was considered uniform) showed the following.

The size at which the electron temperature equalization along and across the magnetic field occurs can be estimated from the theory of dimensions $L_\parallel \approx (\chi_\parallel/n_e)/w_1$ and $L_\perp \approx (\chi_\perp/n_e)/w_1$, where $\chi_{\parallel,\perp}/n_e$ are the thermal conductivity coefficients per electron along and across the magnetic field, and w1 is the energy lost by an electron in collisions per unit time. Furthermore, energy losses at the wall play a significant role in equalizing temperatures in space. In earlier studies, these energies were neglected when calculating spatial plasma density distributions due to the fact that the bulk of the electrons are reflected at the boundary from the resulting potential barrier, equalizing the electron and ion flows to the wall. Calculations showed that using plasma thermal insulation conditions leads to a significantly more uniform electron temperature distribution in space. Examples of calculating the spatial electron temperature distribution are shown in Figure 2.

It was assumed that electron heating occurs in a region of space near the resonator (the resonator center corresponds to the coordinate $z = 0$ in figure 2), and its intensity is independent of the radial coordinate.

Figure 3 shows a similar calculation for the case where heating occurs only in the central region of the plasma with a radius of 1 cm. It is evident that temperature equalization along the radius does not occur, indicating good thermal insulation of the plasma due to the magnetic field.

Figure 4 shows the calculated spatial distribution of the plasma density under the assumption of a constant spatial distribution of the electron temperature. A leveling of the electron density in the central region and a noticeable decrease in the region where the magnetic nozzle begins to form are noticeable.

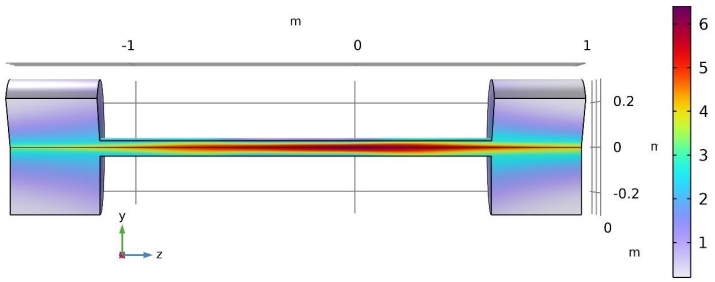

Figure 2. Electron temperature (eV) distribution in space. Energy is deposited uniformly across the cross section. All energy is deposited within a region of $|z| < 10$ cm relative to the resonator center

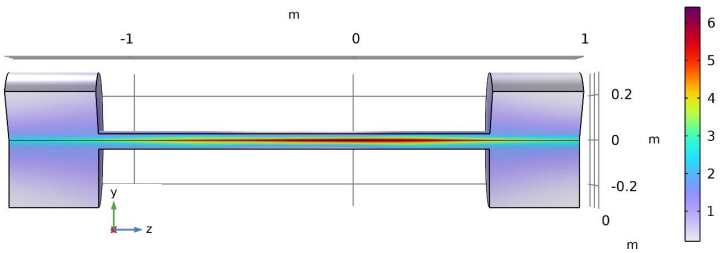

Figure 3. Electron temperature (in relative units) distribution in space. All energy is deposited within a region $|z| < 10$ cm and $|r| < 1$ cm relative to the resonator center

The spatial distribution of the electromagnetic field in the cavity was also calculated (figure 5). In [22], the cavity was excited using a slit in the side wall excited by a waveguide in the center; waves propagating in the azimuthal direction were excited, and the amplitude of the z-component of the electric field was small. In this case, the observed spatial distribution of the field has a more complex structure, with axial components of both the magnetic and electric fields present. Furthermore, various figures suggest the excitation of fields with azimuthal modes $m = 2$, 3, 4, and 5. When calculating the distribution of the electromagnetic field in the plasma near the cavity, the longitudinal distribution of the plasma density was considered constant, since the field is concentrated almost entirely in the region limited by the cavity due to the presence of cutoff waveguides surrounding the quartz tube, where the longitudinal inhomogeneity of the plasma is small.

Azimuthal non-uniformity of the magnetic field energy input may lead to the need to move from solving a two-dimensional axisymmetric problem to solving a three-dimensional one, which will take into account the more complex nature of the movement of charged particles, which is quite possible in a given range of working gas pressures and magnetic field strengths [23–27].

7. Conclusions

1. The paper formulates a simple discharge model based on the solution of the diffusion equations for charged particles, the energy balance equation for electrons, and Maxwell's equations. The solutions are not completely consistent, as the assumptions of uniform plasma heating by the microwave field inside the resonator, equalization of the electron temperature along magnetic

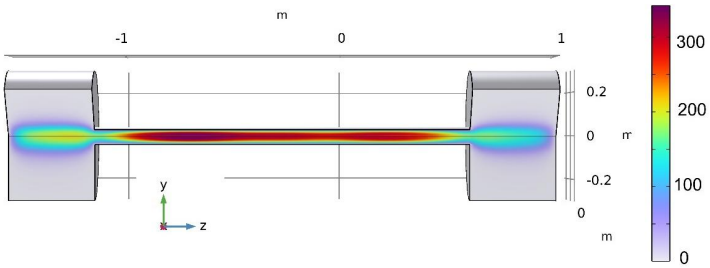

Figure 4. Distribution of electron density (in relative units) in the discharge at a constant electron temperature in space

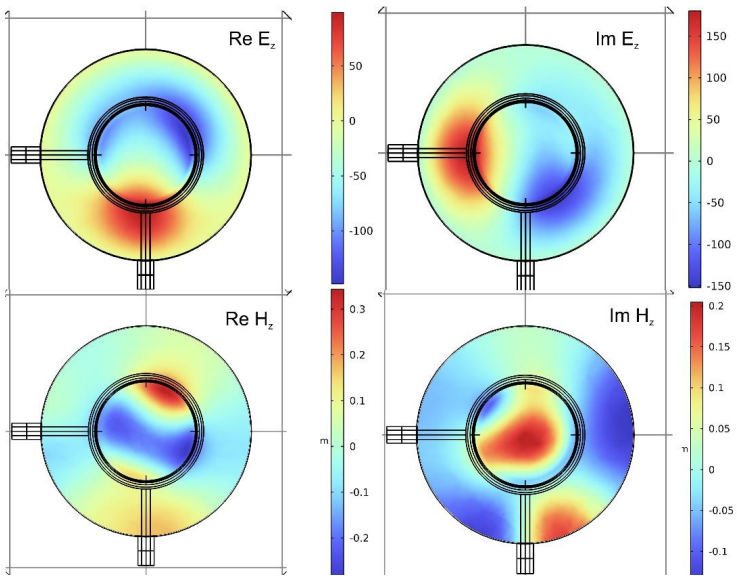

Figure 5. Distribution of the z-component of the electric (V/m) and magnetic (A/m) field in space in the excitation plane of the resonator. Electron density in the center of plasma is equal to 10^{10} cm^{-3}. The ratio of the effective frequency of electron collisions ν to the field frequency ω during calculation is 0.1. In-phase voltages with a frequency of 2.45 GHz and a voltage of 1 V are applied to the rod exciters. In the approximations used, Maxwell's equations are linear for a given electron density distribution, so the fields at other supplied powers increase or decrease proportionally to the gender of the exciting wave

lines, and uniformity of the longitudinal plasma distribution along the quarts pipeline were used to speed up the computation time.

2. Solutions to the heat conduction, diffusion, and Maxwell equations showed that the approximations used are satisfactorily fulfilled in the model under consideration, with the exception of the assumption of azimuthal heating homogeneity. Therefore, to assess the influence of this effect, it is necessary to complicate the model to a fully three-dimensional form.
3. The decrease in electron density near the working chamber may be due to the fact that parts of the field lines in the magnetic nozzle can pass through the boundaries of the quarts pipeline, which increases particle losses in this region.

Author Contributions: Conceptualization, Sergey A. Dvinin and Davlat K. Solikhzoda; methodology, Denis V. Chuprov, Konstantin N. Kornev and Zafari A. Qodirzoda; software, Sergey A. Dvinin and Zafari A. Qodirzoda; validation and visualisation, Konstantin N. Kornev, Zafari A. Qodirzoda; investigation, Sergey A. Dvinin, Zafari A. Qodirzoda, writing—original draft preparation, Sergey A. Dvinin D.V.Chuprov, Davlat K. Solikhzoda; writing—review and editing, Sergey A. Dvinin and Denis V. Chuprov. All authors have read and agreed to the published version of the manuscript.

Funding: The research was carried out with the support of the Ministry of Science and Higher Education of the Russian Federation (State Assignment No. FSSF-2026-0043) within the framework of the federal project "Development of technologies for controlled thermonuclear fusion and innovative plasma technologies".

Data Availability Statement: Data sharing is not applicable.

Conflicts of Interest: The authors declare no conflict of interest.

Declaration on Generative AI: The authors have not employed any Generative AI tools.

References

1. Alton, G. D. & Smithe, D. N. Design studies for an advanced ECR ion source. *Review of Scientific Instruments* **65,** 775–787. doi:10.1063/1.1144954. eprint: https://pubs.aip.org/aip/rsi/article-pdf/65/4/775/19216150/775_1_online.pdf (1994).
2. Asmussen, J., Grotjohn, T., Mak, P. & Perrin, M. The design and application of electron cyclotron resonance discharges. *IEEE Transactions on Plasma Science* **25,** 1196–1221. doi:10.1109/27.650896 (1997).
3. Yonesu, A., Shinohara, S., Yamashiro, Y. & Kawai, Y. Ion and neutral temperatures in an electron cyclotron resonance plasma. *Thin Solid Films* **390.** Proceedings of the 5th Asia-Pacific Conference on Plasma Science & Technology and the 13th Symposium on Plasma Science for Materials, 208–211. doi:10.1016/S0040-6090(01)00921-X (2001).
4. Muta, H., Koga, M., Itagaki, N. & Kawai, Y. Numerical investigation of a low-electron-temperature ECR plasma in Ar/N_2 mixtures. *Surface and Coatings Technology* **171.** Proceedings from the Joint International Symposia of the 6th APCPST, 15th SPSM, 4th International Conference on Open Magnetic Sytems for Plasma Confinement and 11th KAPRA, 157–161. doi:10.1016/S0257-8972(03)00261-5 (2003).
5. Koga, M., Yonesu, A. & Kawai, Y. Measurement of ion temperature in ECR Ar/N2 plasma. *Surface and Coatings Technology* **171.** Proceedings from the Joint International Symposia of the 6th APCPST, 15th SPSM, 4th International Conference on Open Magnetic Sytems for Plasma Confinement and 11th KAPRA, 216–221. doi:10.1016/S0257-8972(03)00274-3 (2003).
6. Kim, S. B., Kim, D. C., Namkung, W., Cho, M. & Yoo, S. J. Design and characterization of 2.45 GHz electron cyclotron resonance plasma source with magnetron magnetic field configuration for high flux of hyperthermal neutral beam. *Review of Scientific Instruments* **81,** 083301. doi:10.1063/1.3477998. eprint: https://pubs.aip.org/aip/rsi/article-pdf/doi/10.1063/1.3477998/15899550/083301_1_online.pdf (Aug. 2010).
7. Jauberteau, J.-L., Jauberteau, I., Cortázar, O. D. & Megía-Macías, A. Langmuir probe in magnetized plasma: Determination of the electron diffusion parameter and of the electron energy distribution function. *Contributions to Plasma Physics* **60,** e201900067. doi:10.1002/ctpp.201900067. eprint: https://onlinelibrary.wiley.com/doi/pdf/10.1002/ctpp.201900067 (2020).
8. Gammino, S. Production of High-Intensity, Highly Charged Ions, 123–164. doi:10.5170/CERN-2013-007.123. arXiv: 1410.7974 (2013).

9. Nakamura, T., Wada, H., Asaji, T. & Furuse, M. Effect of axial magnetic field on a 2.45 GHz permanent magnet ECR ion source. *Review of Scientific Instruments* **87,** 02A737. doi:10.1063/1.4937012. eprint: https://pubs.aip.org/aip/rsi/article-pdf/doi/10.1063/1.4937012/15842829/02a737_1_online.pdf (Dec. 2015).
10. Bogomolov, S. L., Bondarchenko, A. E., Efremov, A. A., *et al.* Production of High-Intensity Ion Beams from the DECRIS-PM-14 ECR Ion Source. *Physics of Particles and Nuclei Letters* **15,** 878–881. doi:10.1134/S1547477118070191 (2018).
11. Gammino, S., Celona, L., Ciavola, G., Maimone, F. & Mascali, D. Review on high current 2.45 GHz electron cyclotron resonance sources (invited)a). *Review of Scientific Instruments* **81,** 02B313. doi:10.1063/1.3266145. eprint: https://pubs.aip.org/aip/rsi/article-pdf/doi/10.1063/1.3266145/13935479/02b313_1_online.pdf (Feb. 2010).
12. Zhang, W. H. *et al.* A 2.45 GHz electron cyclotron resonance proton ion source and a dual-lens low energy beam transporta). *Review of Scientific Instruments* **83,** 02A329. doi:10.1063/1.3669802. eprint: https://pubs.aip.org/aip/rsi/article-pdf/doi/10.1063/1.3669802/15749851/02a329_1_online.pdf (Feb. 2012).
13. Fu, S., Ding, Z., Ke, Y. & Tian, L. Design Optimization and Experiment of 5-cm ECR Ion Thruster. *IEEE Transactions on Plasma Science* **PP,** 1–9. doi:10.1109/TPS.2020.2966662 (Feb. 2020).
14. Lieberman, M. A. & Lichtenberg, A. J. *Principles of Plasma Discharges and Material Processing* (Wiley, New York, 2005).
15. *Comsol Multiphysics. Reference Manual. Comsol Multyphysics. Programming Reference Manual* (2023).
16. Braginsky, S. I. *Transport equations in plasma* in *Problems of Plasma Theory* (ed Leontovich, M. A.) In Russian (1963).
17. Granovsky, V. L. *Electric current in gas, steady-state current* in *General properties of plasma* (ed V. L. Granovsky, A. K. M.) In Russian (Nauka, GRFML, Moscow, 1971).
18. Golyatina, H. V. & Mayorov, S. A. Analytical approximation of collision cross sections of electrons with atoms in inert gases. *Uspekhi Pricladnoy Fisiki* **9.** In Russian, 298–309. doi:10.51368/2307-4469-2021-9-4-298-309 (2021).
19. Alexandrov, A. F., Bogdankevich, L. S. & Rukhadze, A. A. *Principles of Plasma Electrodynamics* doi:10.1007/978-3-642-69247-5 (Springer-Verlag, Berlin, Heidelberg, New York, Tokyo, 1984).
20. *Plasma Electrodynamics* (ed Akhiezer, A. I.) In Russian (Nauka, GRFML, Moscow, 1974).
21. Mironov, V., Bogomolov, S., Bondarchenko, A., Efremov, A., Loginov, V. & Pugachev, D. Three-dimensional modelling of processes in Electron Cyclotron Resonance Ion Source. *Journal of Instrumentation* **15,** P10030. doi:10.1088/1748-0221/15/10/P10030 (2020).
22. Dvinin, S. A. & Korneeva, M. A. Numerical Simulation of the Spatial Structure of the Electromagnetic Field of a Microwave Discharge in a Magnetic Mirror Trap. *Plasma Phys. Rep.* **49,** 1448–1452. doi:10.1134/S1063780X23601438 (2023).
23. Kadomtsev, B. B. & Nedospasov, A. V. Instability of the positive column in a magnetic field and the 'anomalous' diffusion effect. *Journal of Nuclear Energy. Part C, Plasma Physics, Accelerators, Thermonuclear Research* **1,** 230. doi:10.1088/0368-3281/1/4/306 (1960).
24. Nedospasov, A. V. & Khait, V. D. *Oscillations and instabilities of low-temperature plasma* In Russian. 160 pp. (Nauka, GRFML, Moscow, 1979).
25. Nedospasov, A. V. & Khait, V. D. *Fundamentals of Physics of Processes in Devices with Low-Temperature Plasma* In Russian. 224 pp. (Energoatomizdat, Moscow, 1991).
26. Mikhailovsky, A. B. *Plasma Instabilities in Magnetic Traps* In Russian. 296 pp. (Atomizdat, Moscow, 1978).
27. Timofeev, A. V. & Shvilkin, B. N. Drift-dissipative instability of an inhomogeneous plasma in a magnetic field. *Phys. Usp.* **19,** 149–168. doi:10.1070/PU1976v019n02ABEH005134 (1976).

Information about the authors

Dvinin, Sergey A.—Doctor of Physical and Mathematical Sciences, Professor of Lomonosov Moscow State University, leading researcher of Institute of Physical Research and Technology of Peoples' Friendship University of Russia (RUDN University) (e-mail: dvininsa@phys.msu.ru, ORCID: 0000-0002-0163-9282, ResearcherID: J-6595-2012, Scopus Author ID: 6602388907)

Chuprov, Denis V.—Senior Lecturer, Research Associate of Institute of Physical Research and Technology of Peoples' Friendship University of Russia (RUDN University) (e-mail: chuprov-dv@rudn.ru, ORCID: 0000-0002-6768-6196, ResearcherID: O-3193-2013, Scopus Author ID: 6508067157)

Kornev, Konstantin N.—Lead engineer, of Lomonosov Moscow State university, research intern of Institute of Physical Research and Technology of Peoples' Friendship University of Russia (RUDN University) (e-mail: singuliarnost@yandex.ru, ORCID: 0000-0002-7574-566X, Scopus Author ID: 57213826116)

Qodirzoda, Zafari A.—Candidate of Science, Associate Professor of Tajik National University (e-mail: zafar.kodirzoda@yandex.ru, ORCID: 0009-0004-2276-3786, ResearcherID: NMK-4101-2025, Scopus Author ID: 57220783014)

Solikhzoda, Davlat K.—Doctor of Science, Professor of Tajik National University (e-mail: davlat56@mail.ru, ORCID: 0009-0006-8624-3274, Scopus Author ID: 57215526726)

УДК 537.527,533.9.03
PACS 52.80 Pi, 52.80.Sm, 52.50.Sw, 52.40.Db
DOI: 10.22363/2658-4670-2026-34-1-125-138 EDN: UOSEFX

Математические модели разряда низкого давления в магнитном поле, поддерживаемого быстропеременным электромагнитным полем

С. А. Двинин[1,2], Д. В. Чупров[2], К. Н. Корнев[1,2], З. А. Кодирзода[3], Д. К. Солихзода[3]

[1] Российский университет дружбы народов, ул. Миклухо-Маклая, д. 6, Москва, 117198, Российская Федерация

[2] Московский Государственный университет имени М. В. Ломоносова, Ленинские Горы д. 1 стр. 2, Москва, 119991, Российская Федерация

[3] Таджикский национальный университет, Проспект Рудаки, д. 17, Душанбе, 973402, Таджикистан

Аннотация. Разряды использующие электронный циклотронный резонанс (ЭЦР) для нагрева электронов, представляют собой эффективный способ создания плазмы при низком давлении рабочего газа. Цель данной работы — разработка математической модели ЭЦР разряда, реализованного на установке RAPIRA (РУДН), применяемой для реализации целого ряда научных исследований. Эволюция частиц плазма описывается в рамках гидродинамического приближения/ (двумерная модель с цилиндрической симметрией), При расчете пространственного распределения электромагнитного поля используется трехмерная модель холодной плазмы. Расчеты показали, что в рабочем режиме установки (давления газа от $4 \cdot 10^{-4}$ до 10^{-2} Торр, магнитное поле до 2500 Гс) происходит выравнивание температуры электронов вдоль силовых магнитного поля, и в то же время магнитное поле обеспечивает уменьшение потерь энергии на боковые стенки установки. Рассчитаны пространственные распределения плотности и температуры электронов и электромагнитного поля в плазме. Реализованная модель может служить основой для разработки более совершенного набора программных кодов, учитывающих немаксвелловскую природу функции распределения скоростей электронов, обусловленную неадиабатическим характером их нагрева в неоднородном магнитном поле.

Ключевые слова: электронный циклотронный резонанс, ЭЦР-разряд, разряд в резонаторе, разряд в магнитной ловушке, дрейфово-диффузионная модель